Stability and Structure-Forming Properties of the Two Disulfide Bonds of α-Conotoxin GI

Andreas Kaerner and Dallas L. Rabenstein*

Department of Chemistry, University of California, Riverside, California 92521

Received November 9, 1998; Revised Manuscript Received February 17, 1999

ABSTRACT: α-Conotoxin GI is a 13 residue snail toxin peptide cross-linked by Cys2−Cys7 and Cys3−Cys13 disulfide bridges. The formation of the two disulfide bonds by thiol/disulfide exchange with oxidized glutathione (GSSG) has been characterized. To characterize formation of the first disulfide bond in each of the two pathways by which the two disulfide bonds can form, two model peptides were synthesized in which Cys3 and Cys13 (Cono-1) or Cys2 and Cys7 (Cono-2) were replaced by alanines. Equilibrium constants were determined for formation of the single disulfide bonds of Cono-1 and Cono-2, and an overall equilibrium constant was measured for formation of the two disulfide bonds of α-conotoxin GI in pH 7.00 buffer and in pH 7.00 buffer plus 8 M urea using concentrations obtained by HPLC analysis of equilibrium thiol/disulfide exchange reaction mixtures. The results indicate a modest amount of cooperativity in the formation of the second disulfide bond in both of the two-step pathways by which α-conotoxin GI folds into its native structure at pH 7.00. However, when considered in terms of the reactive thiolate species, the results indicate substantial cooperativity in formation of the second disulfide bond. The solution conformational and structural properties of Cono-1, Cono-2, and α-conotoxin GI were studied by ^{1}H NMR to identify structural features which might facilitate formation of the disulfide bonds or are induced by formation of the disulfide bonds. The NMR data indicate that both Cono-1 and Cono-2 have some secondary structure in solution, including some of the same secondary structure as α-conotoxin GI, which facilitates formation of the second disulfide bond by thiol/disulfide exchange. However, both Cono-1 and Cono-2 are considerably less structured than α-conotoxin GI, which indicates that formation of the second disulfide bond to give the Cys2−Cys7, Cys3−Cys13 pairing induces considerable structure into the backbone of the peptide.

The conotoxins are a family of neurotoxic peptides from the venom of marine snails of the genus *Conus* (*1*−*4*). They are highly constrained, basic peptides, 10−30 amino acids in length. A characteristic feature of the conotoxins is the presence of conserved cysteine residues that form distinctive disulfide frameworks. The disulfide framework varies among the different conotoxins and is responsible for maintaining a fully active tertiary structure. The first conotoxin to be isolated and characterized was α-conotoxin GI, a 13 amino acid peptide which is cross-linked by two intrachain disulfide bonds, one linking Cys2 and Cys7 and the other Cys3 and Cys13 (5). α-Conotoxin GI causes paralysis by antagonism of acetylcholine binding to the nicotinic acetylcholine receptor of the neuromuscular junction (*3*). Because of the selectivity of its binding, α-conotoxin GI is a useful neuropharmacological tool for studying binding and signal transduction at the nicotinic acetycholine receptor.

As part of a program to characterize the role of disulfide bonds in small bioactive peptides (*6, 7*), we are investigating the stability and structure-inducing properties of the disulfide bonds in several conotoxin peptides. In this paper, we report the results of studies on α-conotoxin GI. Our objective in this study is to characterize the contribution each disulfide bond makes to the stability of the disulfide framework of α-conotoxin GI and to identify structural features which either facilitate formation of or are induced by formation of the disulfide bonds. To investigate the stabilities of the individual disulfide bonds, we synthesized two peptides in which either Cys3 and Cys13 or Cys2 and Cys7 are replaced by alanine as models for the one-disulfide intermediates which form on the folding pathway of α-conotoxin GI. The amino acid sequences of α-conotoxin GI and the two model peptides, Cono-1 and Cono-2, are shown in Figure 1. The stabilities of the disulfide bonds in Cono-1 and Cono-2 and the stability of the disulfide framework of α-conotoxin GI were characterized in terms of equilibrium constants for their formation by thiol/disulfide exchange reactions with glutathione, both in pH 7.00 phosphate buffer and in pH 7.00 buffer plus 8 M urea. Glutathione (GSH) was chosen for this study because equilibrium constants for its thiol/disulfide exchange reactions with a variety of other biological thiols are available for comparison, GSH is the standard to which other thiols and disulfides are compared thermodynamically (*8*), and the formation of the disulfide bond of oxidized glutathione (GSSG) is not affected by the presence of urea (*9*). To identify the structural features induced by the disulfide bonds, the conformational properties of the reduced

† This research was supported in part by National Instututes of Health Grant GM 37000. Funding for the Varian Unity *Inova* 500 Spectrometer was provided in part by NSF-ARI Grant 9601831.

* To whom correspondence should be addressed. E-mail: dlrab@mail.ucr.edu. Fax: 909-787-4713.

10.1021/bi9826658 CCC: $18.00
Published on Web 04/01/1999

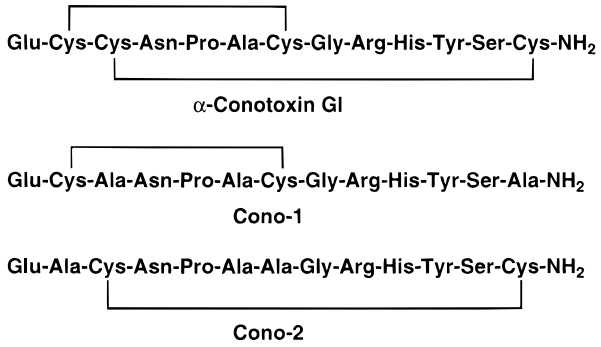

FIGURE 1: Peptide sequences of α-conotoxin GI and the two models for the single disulfide intermediates Cono-1 and Cono-2.

and the disulfide forms of Cono-1 and Cono-2 and of α-conotoxin GI in pH 7.00 phosphate buffer and in buffer plus 8 M urea were characterized by 1D and 2D ^{1}H NMR. The solution structure of α-conotoxin GI has been determined by NMR (*10*−*13*) and its structure in the solid state has been determined by X-ray crystallography (*14*).

MATERIALS AND METHODS

Chemicals. The 9-fluorenylmethoxycarbonyl (Fmoc) protected amino acids, 1-hydroxybenzotriazole (HOBt), 1-hydroxy-7-azabenzotriazole (HOAt), and 20% piperidine in *N*,*N*-dimethylformamide (DMF), were obtained from Millipore Corp. The [[5-(4′-Fmoc-aminomethyl-3′,5′-dimethoxy phenoxy) valeric acid]poly(ethylene glycol)polystyrene] (Fmoc-PAL-PEG-PS) resin with an approximate loading capacity of 0.20 mmol/g was purchased from Millipore or Nova Biochem. *N*,*N*′-diisopropylcarbodimide (DIPCDI), glutathione (free acid), and oxidized glutathione (disodium salt) were obtained from Sigma Chemical Co. Deuterated dithiothreitol was purchased from Isotec.

Peptide Synthesis. α-Conotoxin GI, Cono-1, and Cono-2 were synthesized using solid-phase Fmoc peptide synthesis methodology on a Millipore model 9050 plus peptide synthesizer. After each amino acid coupling, the Fmoc group was removed from the N-terminal amino group of the resin bound peptide with 20% piperidine in DMF at a flow rate of 10 mL/min for three min. Incoming amino acids were preactivated for 6 min with HOBt or HOAt and DIPCDI and couplings were run for 120 min (*15*, *16*). Double couplings were used to increase the coupling efficiency of difficult couplings. After each coupling, the peptide on the resin was reacted with capping reagent (15% acetic anhydride and 5% HOBt in DMF) for 5 min to cap unreacted amino groups. The peptides were cleaved from the resin and deprotected with a cleavage cocktail consisting of 88% trifluoroacetic acid, 5% H_2O, 5% phenol, and 2% triisopropylsilane (cocktail B) (*17*). The crude peptides were purified by reversed-phase HPLC using a Bio-Rad model 2800 HPLC system equipped with a Linear model 205 dual wavelength UV detector and a 250 mm by 10 mm Vydac column packed with a 5 μm diameter, 300 Å pore size C18 stationary phase. The two channels of the detector were set to 215 and 280 nm to detect absorbance due to the peptide bonds and aromatic-containing compounds, respectively. The peptides were eluted with a two solvent gradient consisting of 0.1% w/w TFA in H_2O and 0.1% w/w TFA in acetonitrile. The crude peptide was dissolved in a mixture of the two solvents, together with a 20-fold excess of DTT to reduce any disulfide bonds formed during isolation of the crude peptide. To ensure complete reduction by DTT, the pH was raised to 7 for approximately 10 min.

Cono-1 and Cono-2 were synthesized using Fmoc-protected cysteine with the side chain blocked with the trityl (Trt) protecting group, which is removed by the cleavage cocktail. After isolation of the reduced dithiol forms of Cono-1 and Cono-2 by HPLC, they were converted to the disulfide form by reaction with DMSO (*18*, *19*). The peptides were dissolved in pH 3 solution at a concentration ranging from 100 to 300 μM, the pH was increased slowly to 8, and then DMSO was added to a final concentration of 1% v/v. The solution was allowed to react for 10−12 h and lyophilized, and the oxidized peptide was obtained from the lyophilized mixture by HPLC.

To ensure the correct cysteine pairing (Cys2−Cys7 and Cys3−Cys13) in α-conotoxin GI, an orthogonal procedure similar to that reported in the synthesis of α-conotoxin SI was used to form the two disulfide bonds (*20*). Since formation of the Cys2−Cys7 disulfide bond first gave better yields for α-conotoxin SI, this strategy was also used in the synthesis of α-conotoxin GI. Cys2 and Cys7 were protected with the acid labile Trt group, while Cys3 and Cys13 were protected with the S-acetamidomethyl (Acm) group, which is stable to both acidic and basic conditions. After cleavage and deprotection with cocktail B, the Cys2−Cys7 disulfide bond was formed by reaction with DMSO and the intermediate peptide was isolated by HPLC. The Cys3−Cys13 disulfide bond was then formed by oxidation with I_2 or with $Tl(TFA)_3$, both of which remove the ACM protecting group as part of the oxidation step.

For all peptides, the electrospray mass spectrum was used for verification of molecular mass, and the purity of each peptide was checked using capillary electrophoresis (CE). Typical conditions for the CE separations were a pressure injection of 5 psi/s, a separation voltage of 10 kV, UV detection at 215 nm, and a pH 2.5 phosphate buffer with a polyacrylamide polymer additive (Bio-Rad). The peptides were dissolved in the degassed phosphate buffer solution. At the pH of the buffer, the peptides are positively charged and thus the CE instrument was run with the detector maintained at a lower potential than the injection end. In all cases, a single peak was obtained in both the HPLC chromatogram and the CE electropherogram for the purified peptides.

Measurement of Thiol/Disulfide Exchange Equilibrium Constants. Equilibrium constants were determined for thiol/disulfide exchange reactions of Cono-1, Cono-2, and α-conotoxin GI with glutathione. Equilibrium mixtures were analyzed by HPLC using a Bio-Analytical Systems (BAS) model 200 HPLC, equipped with a 3.2 mm × 100 mm C18 reversed-phase column, a dual channel Linear Instruments model 204 UV detector and an Alcott auto sampler. The detector was set to 275 nm. The separations were carried out under isocratic conditions using a H_2O/acetonitrile mobile phase containing 0.1 M TFA. The pH of the mobile phase was adjusted to 2.5 with NaOH. The optimum acetonitrile content for good separation with reasonable elution times was found to be 11.5% for Cono-1 and Cono-2 and 11.8% for α-conotoxin GI.

Equilibrium solutions were prepared in buffer containing 0.1 M phosphate, 0.1 M NaCl, and 1 mM EDTA at pH 7.00 and 25 °C under a nitrogen atmosphere in a glovebag. The procedure generally involved reacting Cono-1, Cono-2, or α-conotoxin GI in the fully reduced form with a GSH/GSSG redox buffer. The concentration of the GSH/GSSG buffer was in the 800 μM to 34 mM range, and the concentration of peptide was in the range 30−120 μM. Sample volumes of 300 μL were transferred to autoinjector vials, which were sealed in the glovebag with silicon-PTFE-silicon layered septa. The layered septa reseal after being pierced with a needle so that an anaerobic environment was maintained in the vial as replicate injections were made onto the HPLC with the auto sampler. The concentrations of Cono-1 and Cono-2 in the reduced, oxidized, and mixed disulfide forms were determined from peak areas in the chromatogram measured at 275 nm. Samples were quenched by lowering the pH to <3.0 by addition of 1 M HCl prior to HPLC analysis. The response of the detector was calibrated using reduced peptide; the calibration curves were linear over the concentration range 5−140 μM, which covers the concentration range used in these experiments.

NMR Spectroscopy. One- and two-dimensional NMR spectra were measured at 500 MHz using either a Varian VXR-500S spectrometer or a Varian Unity-Inova spectrometer. Samples were contained in NMR tubes obtained from Norell, Inc. or from Shigemi Co., Inc. The Shigemi tubes were used to improve elimination of the water resonance by the presaturation method. Peptide samples were dissolved in either 90% H_2O/10% D_2O or 90% H_2O/10% D_2O plus 8 M urea. Deuterated DTT was added to NMR solutions of the reduced peptide. The water resonance was suppressed in all 1D and 2D experiments with a presaturation pulse.

Two-dimensional spectra, including total correlation spectroscopy (TOCSY), rotating frame Overhauser effect spectroscopy (ROESY), and nuclear Overhauser effect spectroscopy (NOESY) spectra, were measured with standard pulse sequences. Typically, spectra were measured with 4K points in the directly detected (F2) dimension and 128, 256, or 512 points in the indirectly detected (F1) dimension, depending on the necessary digital resolution. The F1 dimension was zero filled to 4K points. Quadrature detection in the F1 dimension was achieved using the hypercomplex method (*21*). Two-dimensional NMR data were generally processed with a 90° shifted sinebell squared apodization function in both the F1 and F2 dimensions and baseline correction was applied after the first (t2) transforms.

The ^{1}H NMR spectra for the reduced and oxidized forms of Cono-1, Cono-2, and α-conotoxin GI were assigned by a procedure which involved first assignment of amide NH resonances to types of amino acids using the fingerprint patterns of cross-peaks in the TOCSY spectrum of the peptide. The position of each amino acid in the sequence, e.g., each of the cysteine residues identified in the TOCSY spectrum, was then established using through space $NH_i-C_\alpha H_i$ and $C_\alpha H_i-NH_{i+1}$ connectivities obtained from NOESY and ROESY spectra.

Measurement of Acid Dissociation Constants. Acid dissociation constants were determined for each of the titratable groups of Cono-1, Cono-2, and α-conotoxin GI, including the two cysteine thiol groups of Cono-1 and Cono-2 and the four cysteine thiol groups of α-conotoxin GI, from the pH dependence of the chemical shifts of resonances for carbon-bonded protons located near each titratable group. Because of extensive overlap of resonances for the cysteines in 1D spectra, chemical shift titration data for the cysteines were measured from 1D subspectra which were obtained from 2D TOCSY spectra, as described previously (*22*). NMR measurements were made on 5 mM peptide in 90% H_2O/10% D_2O at 25 °C. A total of 8K data points were collected at 256 t1 increments in the TOCSY experiment using a mixing time of 120 ms; 24 transients were collected at each t1 increment. The pH was measured directly in the NMR tube using an Ingold combination ultramicroelectrode. No correction was made for isotope effects. Acid dissociation constants were determined as mixed activity-concentration constants (activity of hydrogen ion, concentration of acidic group and its conjugate base).

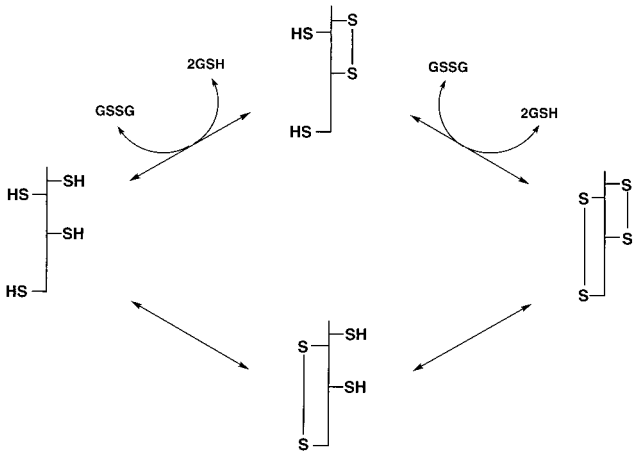

FIGURE 2: Stepwise reaction sequence for formation of the native disulfide bonds of α-conotoxin GI by thiol/disulfide exchange with GI.

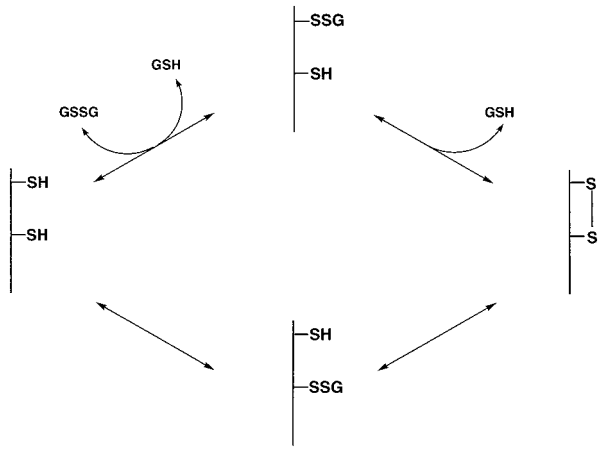

FIGURE 3: The stepwise reaction sequence for formation of the disulfide bonds in Cono-1 and Cono-2.

The chemical shift observed for carbon-bonded protons located near a titratable group, δ_{obs} is given by eq 1:

$$\delta_{obs} = f_{HA}\delta_{HA} + f_A\delta_A \quad (1)$$

where f_{HA} and f_A represent mole fractions and δ_{HA} and δ_A the chemical shifts of the carbon-bonded protons when the titratable group is in the acid and conjugate base forms, respectively. Acid dissociation constants were obtained by

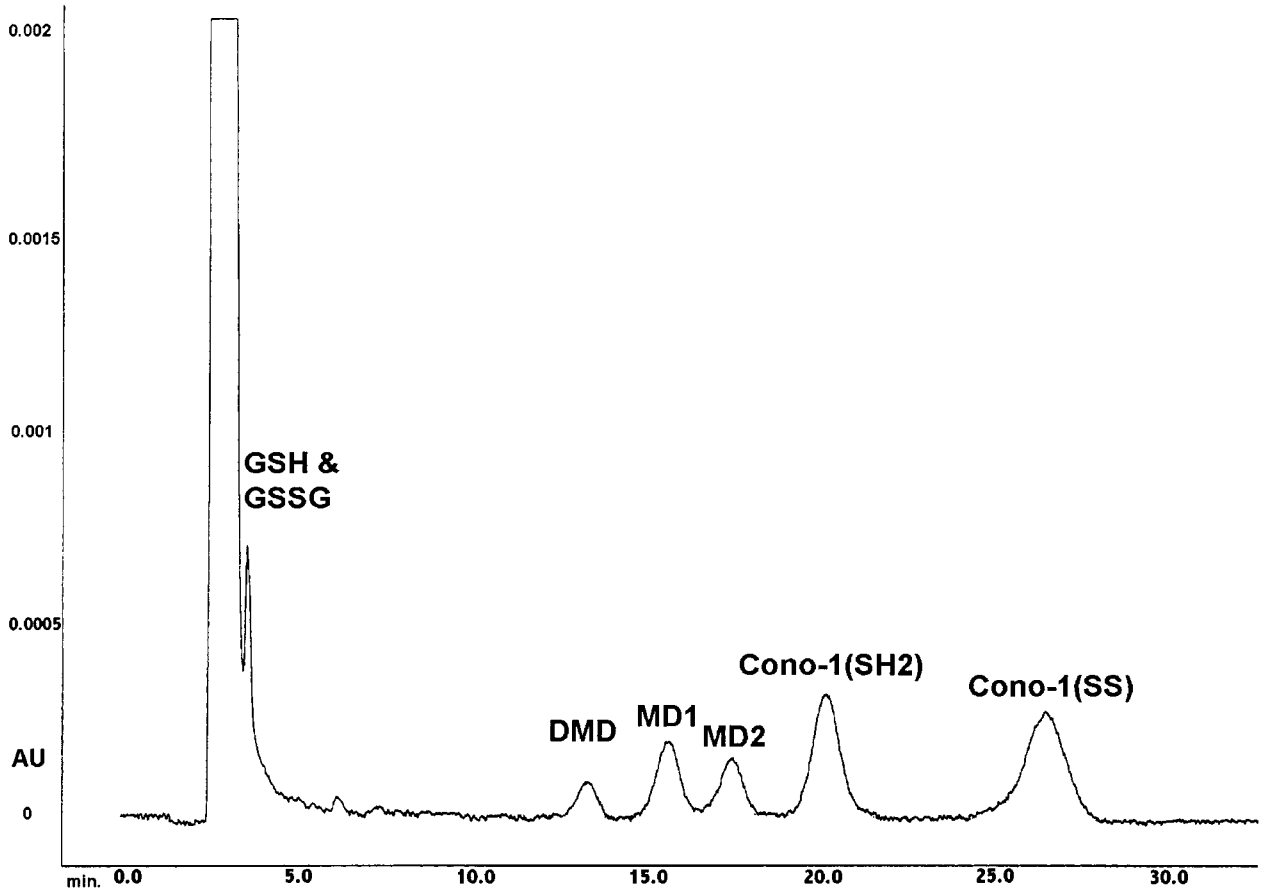

FIGURE 4: Chromatogram of an equilibrium mixture of Cono-1 plus GSH/GSSG redox buffer. The initial concentrations were 71.2 μM reduced Cono-1, 9.74 mM GSH and 1.89 mM GSSG at pH 7.00 and 25 °C. The separation conditions and the peak labels are given in the text.

a three-parameter (δ_{HA}, δ_A, and K_A) fit of chemical shift-pH titration data to eq 2:

$$\delta_{obs} = \frac{a_{H^+}\delta_{HA} + K_A\delta_A}{a_{H^+} + K_A} \quad (2)$$

using the computer program *Scientist* from Micromath Scientific software. Equation 2 is obtained from eq 1 by expressing f_{HA} and f_A in terms of K_A.

RESULTS

The overall reaction sequence for formation of the disulfide bonds of α-conotoxin GI by thiol/disulfide exchange with oxidized glutathione is shown in Figure 2. In the first step, GSSG reacts with the fully reduced form of α-conotoxin GI to form either the Cys2−Cys7 or the Cys3−Cys13 disulfide bond. The single disulfide intermediates in turn react with another GSSG to form the second disulfide bond. Not shown in the overall reaction sequence are the α-conotoxin GI-GSH mixed disulfides which form as intermediates in each step and the single and double disulfide-containing α-conotoxin GI species which form from mispairing of the cysteine residues. Because the two single disulfide intermediates shown in Figure 2 are present in low abundance, the single disulfide analogues Cono-1 and Cono-2 were used as models for these intermediates. This strategy has also been used to study the folding pathways of apamin (*23*−*25*).

Equilibrium Constants for Thiol/Disulfide Exchange. The stepwise reaction sequence for formation of the disulfide bonds in Cono-1 and Cono-2, including the mixed disulfide intermediates, is shown in Figure 3. Not shown in Figure 3 is the double mixed disulfide which can form by reaction of the single mixed disulfides with another molecule of GSSG. The two stepwise equilibrium constants and the overall equilibrium constant for the formation of the disulfide bonds in Cono-1 and Cono-2 are defined by eqs 3−5, where Cono(SH2) and Cono(SS) represent the peptides in the reduced and disulfide forms and MD1 and MD2 the two peptide-GSH mixed disulfides.

$$K_1 = \frac{[\text{MD1} + \text{MD2}][\text{GSH}]}{[\text{Cono(SH2)}][\text{GSSG}]} \quad (3)$$

$$K_2 = \frac{[\text{Cono(SS)}][\text{GSH}]}{[\text{MD1} + \text{MD2}]} \quad (4)$$

$$K_3 = \frac{[\text{Cono(SS)}][\text{GSH}]^2}{[\text{Cono(SH2)}][\text{GSSG}]} \quad (5)$$

The overall equilibrium constant for formation of the two disulfide bonds of α-conotoxin GI is defined by eq 6,

$$K_{ov} = \frac{[\text{α-conotoxin GI}][\text{GSH}]^4}{[\text{α-conotoxin GI(SH4)}][\text{GSSG}]^2} \quad (6)$$

Equilibrium constants were determined using concentrations obtained from HPLC analysis of equilibrium mixtures. To illustrate, the chromatogram for an equilibrium mixture of Cono-1 with GSH and GSSG is shown in Figure 4. The

Table 1: Equilibrium Constants for Thiol/Disulfide Exchange Reactions of Cono-1, Cono-2, and α-Conotoxin GI with Glutathione[a,b]

	Cono-1	Cono-2	α-Conotoxin GI
K_1	5.3 ± 0.4	5.3 ± 1.0	
K_2 (M)	0.015 ± 0.001	0.015 ± 0.003	
K_3 (M)	0.077 ± 0.009	0.079 ± 0.018	
K_{ov} (M^2)			0.020 ± 0.007
$E^{o\prime}$ (V)[c]	−0.229 ± 0.001	−0.229 ± 0.003	−0.237 ± 0.003

[a] 0.1 M phosphate, 0.1 M NaCl, 1 mM EDTA, pH 7.00, 25 °C. [b] The number of samples was 23 for Cono-1, 19 for Cono-2, and 12 for α-Conotoxin GI. [c] Relative to the standard hydrogen electrode (SHE).

Table 2: Equilibrium Constants for Thiol/Disulfide Exchange Reactions of Cono-1,Cono-2 and α-Conotoxin GI with Glutathione under Denaturing Conditions[a,b]

	Cono-1	Cono-2	α-Conotoxin GI
K_1	4.6 ± 0.5	4.6 ± 0.8	
K_2 (M)	0.016 ± 0.002	0.011 ± 0.001	
K_3 (M)	0.074 ± 0.008	0.050 ± 0.007	
K_{ov} (M^2)			0.0087 ± 0.0003
$E^{o\prime}$ (V)[c]	−0.229 ± 0.002	−0.224 ± 0.002	−0.232 ± 0.002

[a] 0.1 M phosphate, 0.1 M NaCl, 1 mM EDTA, 8 M urea, pH 7.00, 25 °C. [b] The number of samples was 21 for Cono-1, 19 for Cono-2, and 14 for α-Conotoxin GI. [c] Relative to the standard hydrogen electrode (SHE).

peaks for the reduced and oxidized forms of Cono-1 were assigned using retention times for pure samples of each. The peaks for the two single mixed disulfides and the double mixed disulfide (DMD) were identified by the dependence of peak areas on the concentrations and concentration ratios of GSSG and GSH (*6*).

The equilibrium constants determined for Cono-1 and Cono-2 are reported in Table 1. Each reported equilibrium constant is the result of measurements made on multiple equilibrium samples, as indicated in the footnote to the table, and replicate measurements were made on each sample. To verify that the reactions are reversible, equilibrium was established as indicated by no change in HPLC peak areas with time. Then, additional GSH was added to shift the equilibrium and the solution reanalyzed by HPLC until a new equilibrium was established. The equilibrium constants obtained from the two equilibrium conditions were the same within experimental error. For example, values of 5.0, 0.016, and 0.085 M were obtained for K_1, K_2, and K_3, respectively, from the reaction of 59.4 μM reduced Cono-1 with 9.74 mM GSH and 2.83 mM GSSG. After equilibrium was reestablished following the addition of more GSH to give 21.10 mM GSH and 1.89 mM GSSG, values of 5.6, 0.016, and 0.087 M were obtained.

The values determined for K_{ov} for α-conotoxin GI are also reported in Table 1.

The equilibrium constants were also determined for Cono-1, Cono-2, and α-conotoxin GI in pH 7.00 phosphate buffer plus 8 M urea. The results are reported in Table 2.

NMR Structural Studies. Structure-sensitive ^{1}H NMR parameters, including NOE cross-peak intensities in ROESY and NOESY spectra, $^3J_{NH-C\alpha H}$ coupling constants, the chemical shifts of the amide NH and CαH resonances, and the temperature dependence of the chemical shifts of the amide NH resonances, were measured for the reduced and disulfide forms of Cono-1, Cono-2, and α-conotoxin GI at pH 2.00 in 90% H_2O/10% D_2O and 90% H_2O/10% D_2O plus 8 M urea solutions. The ^{1}H NMR spectra were assigned as described above; chemical shift data are reported in the Supporting Information for this article. For most of the peptides, single resonances were observed for specific protons, indicating that the peptide exists as either a single conformation in solution or is in rapid interchange on the NMR time scale among two or more conformations. However, for several of the peptides, including the disulfide form of Cono-1, additional resonances were observed in the spectrum, as illustrated by the amide NH region of the spectrum of Cono-1 in Figure 5. The less intense resonances, indicated by asterisks, were assigned to the amide NH protons of peptide in which the Asn4−Pro5 peptide bond has the cis conformation (*26*).

Of the structure-sensitive parameters listed above, the NOEs provide the most information about peptide secondary structure. Some of the NOEs obtained from ROESY spectra for the disulfide forms of Cono-1, Cono-2, and α-conotoxin GI in 90% H_2O/10% D_2O solution are summarized in Figure 6, where the line thickness is proportional to the intensity of the NOE cross-peak. In addition, the following weak to very weak long-range NOEs were observed in ROESY spectra measured at 16 °C using a 200 ms mixing time. For Cono-1, Asn4$^{\beta}$−Cys7^{NH}, Asn4$^{\beta}$−Gly8^{NH}, Pro5$^{\alpha}$−Gly8^{NH}, Pro5$^{\alpha}$−Arg9^{NH}, Tyr11^{3,5}−Ala13$^{\beta}$; for Cono-2, Asn4$^{\epsilon NH}$−

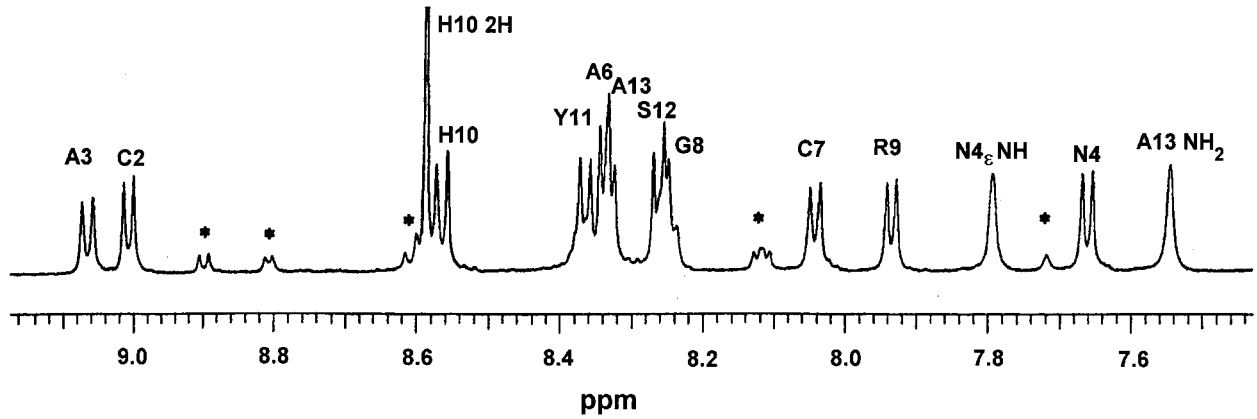

FIGURE 5: The amide NH region of the 500 MHz ^{1}H NMR spectrum of 6.5 mM oxidized Cono-1 in 90% H_2O/10% D_2O at pH 2.00 and 16 °C. The resonances marked with an asterisk are for amide NH protons of peptide in which the Asn4−Pro5 peptide bond has the cis conformation.

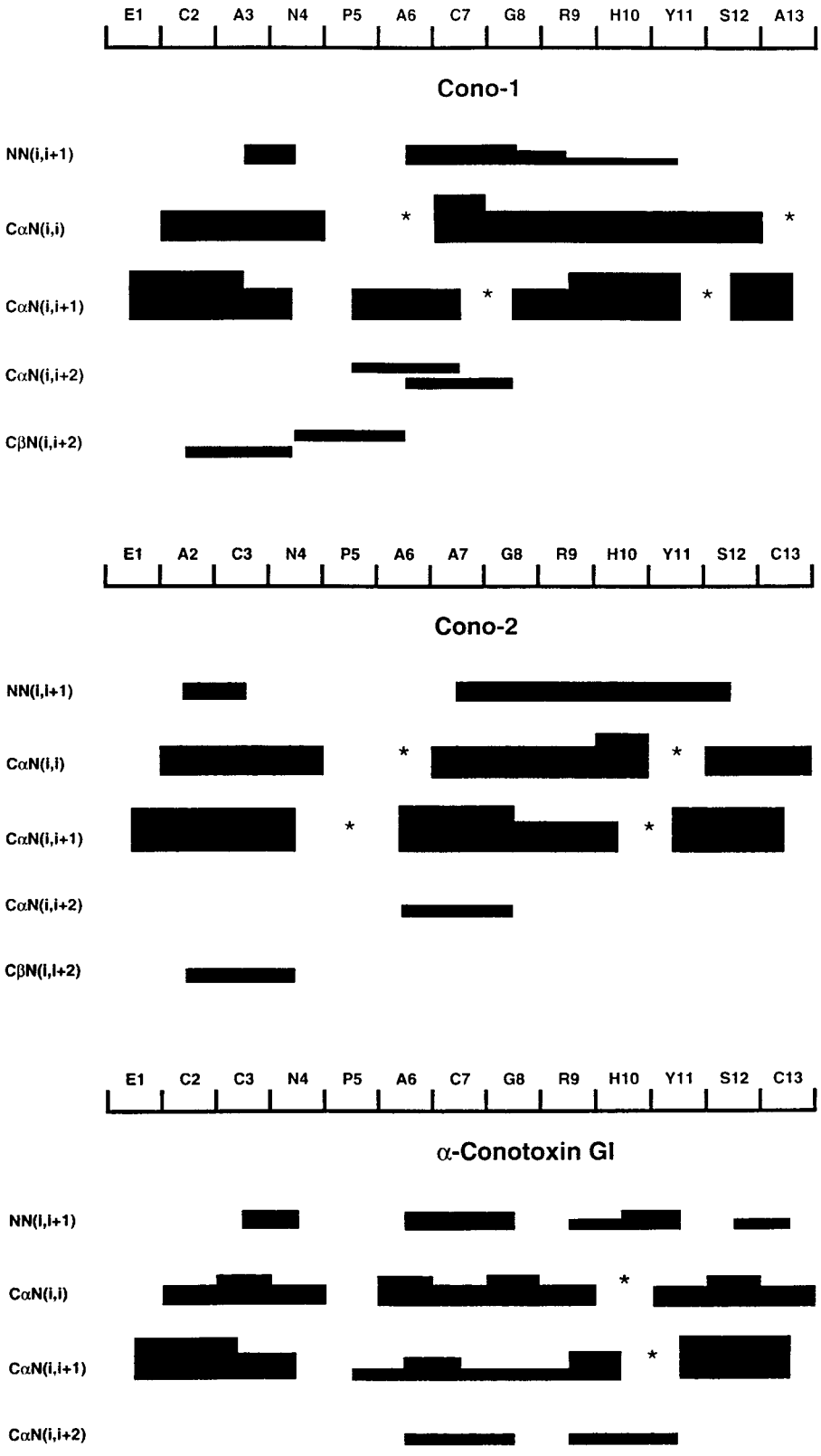

FIGURE 6: Plots of NOEs from ROESY spectra for the disulfide forms of Cono-1 (top), Cono-2 (middle), and α-conotoxin GI (bottom) in 90% H_2O/10% D_2O at pH 2.00 and 16 °C. The intensity of the cross-peaks is proportional to the thickness of the lines. The asterisks indicate resonance overlap.

Ala6$^{\beta}$, either Pro5$^{\alpha}$−Tyr11^{2,6} or Ala6$^{\alpha}$−Tyr11^{2,6}, either Pro5$^{\alpha}$−Tyr11^{3,5} or Ala6$^{\alpha}$−Tyr11^{3,5}, Ala7$^{\beta}$−Tyr11^{2,6}, Arg9$^{\delta}$−Tyr11^{3,5} and Tyr11^{3,5}−Cys13$^{\beta}$; and for α-conotoxin GI, Glu1$^{\gamma}$−Cys3^{NH}, Cys2$^{\beta}$−Ser12^{NH}, Cys2^{NH}−Ser12$^{\beta}$, Cys3^{NH}−Tyr11^{2,6}, Cys3$^{\alpha}$−Tyr11^{3,5}, Asn4$^{\beta}$−Ala6^{NH}, Asn4^{NH}−Tyr11^{3,5}, Asn4^{NH}−Tyr11^{2,6}, Asn4$^{\epsilon NH}$−Cys13$^{NH-terminal}$, Cys7$^{\beta}$−Tyr11^{2,6}, Tyr11^{2,6}−Cys13^{NH}, Tyr11^{3,5}−Cys13^{NH} and Tyr11^{3,5}−Cys13$^{\beta}$.

Amide NH_i−NH_{i+1}, $C\alpha H_i$−NH_i, and $C\alpha H_i$−NH_{i+1} NOEs were observed for the reduced forms of Cono-1, Cono-2,

FIGURE 7: Plots of the amide NH_i-NH_{i+1} NOEs from ROESY spectra for the reduced forms of Cono-1, Cono-2, and α-conotoxin GI in 90% H_2O/10% D_2O at pH 2.00 and 16 °C. The intensity of the cross-peaks is proportional to the thickness of the lines.

Table 3: Temperature Dependence of the Chemical Shifts of the Amide NH Resonances for the Conotoxin Peptides.[a,b,c]

	Cys2	Cys3	Asn4	Ala6	Cys7	Gly8	Arg9	His10	Tyr11	Ser12	Cys13
Cono-1[d]	6.6	8.7	2.5	4.1	2.5	5.1	4.6	7.8	7.7	6.1	8.8
Cono-2[e]	6.8	8.1	7.5	5.2	6.2	7.3	6.8	7.3	4.4	8.1	0.0
α-Conotoxin GI	5.1	5.3	2.5	2.6	1.2	2.7	10.8	3.1	1.9	4.8	9.0
reduced Cono-1[d]	5.9	8.7	8.6	7.0	6.7	6.3	6.5	7.8	8.2	6.1	8.8
reduced Cono-2[e]	6.6	8.2	8.5	6.6	6.8	7.6	6.1	7.6	8.0	6.5	7.7
reduced α-Conotoxin GI	5.0	7.1	7.7	7.6	7.8	7.2	7.0	9.1	8.3	7.0	8.3

[a] 90% H_2O/10% D_2O, pH 2.00. [b] Pro5 does not have an amide proton and Glu1(NH) is not observed due to exchange with solvent. [c] Values are negative and have units of parts per billion per degree Celsius. [d] Cys3 and Cys13 are replaced by Ala. [e] Cys2 and Cys7 are replaced by Ala.

and α-conotoxin GI; however, no longer range NOEs were observed. The amide NH_i-NH_{i+1} NOEs observed for the peptides in their reduced forms are summarized in Figure 7.

The values measured for $^3J_{NH-C\alpha H}$ are in the range 5.0−7.9 Hz for all three peptides in the reduced form and for the disulfide forms of Cono-1 and Cono-2. For the disulfide form of α-conotoxin GI, the values for $^3J_{NH-C\alpha H}$ are in this range except for Cys3 (9.1 Hz), Cys7 (4.4 Hz), His10 (8.8 Hz), Tyr11 (4.0 Hz), and Cys13 (8.4 Hz). The temperature dependence of the chemical shifts of the amide NH resonances is reported in Table 3.

The chemical shifts of resonances for the amide NH and CαH protons of amino acids located in regions of secondary structure tend to be different from those of amino acids in random coil peptides (*27*). The differences between the amide NH and the CαH chemical shifts at pH 2.00 and 16 °C in 90% H_2O/10% D_2O and 90% H_2O/10% D_2O plus 8 M urea are presented in Figures 8 and 9, respectively.

Cis/Trans Isomers of the Asn4−Pro5 Peptide Bond. The less intense resonances in the amide NH region of the 1D spectrum of Cono-1 (Figure 5) were assigned to peptide in which the Asn4−Pro5 peptide bond has the cis conformation. The assignment to the cis conformation was made using TOCSY and ROESY data, as described previously for vasopressin and oxytocin (*26*). Specifically, two sets of cross-peaks were observed for proline in a TOCSY spectrum measured at 16 °C, a strong set for proline in a major abundance species and a weak set for proline in a minor abundance species. The major abundance species has a trans Asn4−Pro5 peptide bond, as indicated by a cross-peak between CαH of Asn4 and $C_\delta H_2$ of Pro5 in a ROESY spectrum also measured at 16 °C. The CαH resonance for proline of the minor abundance species has a ROESY cross-peak to CαH of a minor abundance asparagine, providing direct evidence for a cis Asn−Pro peptide bond. The minor and major abundance species are proven to be two conformations of the same molecule by an exchange cross-peak between the CαH resonances for the two conformations in a ROESY spectrum measured at 65 °C. ROESY exchange cross-peaks are also observed between pairs of weak and strong amide resonances (Figure 10). Exchange cross-peaks have the same phase as diagonal peaks in the ROESY spectrum, but are opposite in phase to through space dipolar cross-peaks (*28*). Only the cross-peaks in phase with the diagonal are plotted in Figure 10. Exchange cross-peaks are observed for the amide NH protons of Ala3, Asn4, Ala6, Cys7, and Arg9, i.e., the amide NH protons of amino acids which are reasonably close to the Asn4−Pro5 peptide bond.

From the intensities of resonances for the cis and trans conformations in the amide NH region (Figure 5), the population of the cis isomer is determined to be 16.3% at 16 °C for oxidized Cono-1. The conformation of the cis isomer was determined to be less than 2% for the reduced forms of Cono-1 and α-conotoxin GI and for Cono-2 in both the reduced and oxidized forms. A second conformation was detected for native α-conotoxin GI, at a population of ∼3.3%. It was not possible to establish the identity of this isomer because of its very low concentration, but data suggests it also has the Asn4−Pro5 peptide bond in the cis conformation.

Determination of Acid Dissociation Constants. Acid dissociation constants were determined for each titratable group of the reduced forms of Cono-1, Cono-2, and α-conotoxin GI from the pH dependence of the chemical shifts of adjacent carbon-bonded protons. The results are reported in Table 4.

DISCUSSION

Formation of the Disulfide Bonds of α-Conotoxin GI. The Cys2−Cys7 and Cys3−Cys13 disulfide bonds stabilize the globular three-dimensional structure of α-conotoxin GI (*10*−*14*). This native pairing of cysteine residues predominates

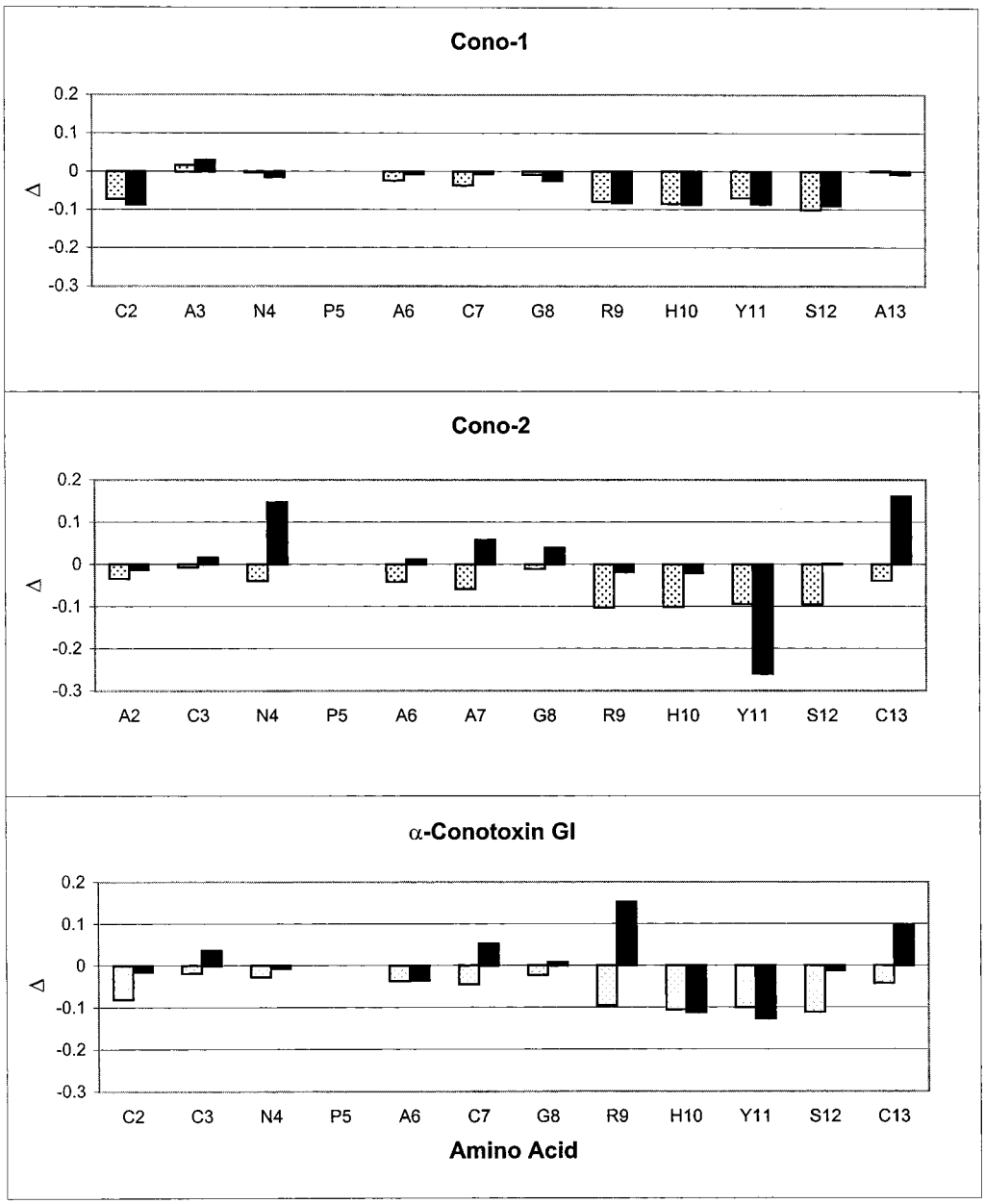

FIGURE 8: The difference between the chemical shifts of the amide NH resonances of the reduced (stipled) and disulfide (black) forms of Cono-1, Cono-2, and α-conotoxin GI in 90% H_2O/10% D_2O and 90% H_2O/10% D_2O plus 8 M urea ($\Delta = \delta_{\text{no urea}} - \delta_{\text{urea}}$). pH 2.00 and 16 °C.

in oxidative folding experiments, e.g., 71% of the product from reaction of the fully reduced peptide with GSSG has the native disulfide pairing (*29*), which suggests some degree of cooperativity in the disulfide bond formation and folding process.

As shown in Figure 2, there are two stepwise pathways by which the native disulfide bonds of α-conotoxin GI can form by reaction with GSSG. The two steps of each pathway have been quantitatively characterized in terms of equilibrium constants for formation of the disulfide bonds by thiol/disulfide exchange. The first steps of the two pathways were characterized using Cono-1 and Cono-2 as models for the one disulfide intermediates in the folding pathway. Equilibrium constants of 0.077 and 0.079 M were determined for formation of the Cys2−Cys7 and Cys3−Cys13 disulfide bonds in Cono-1 and Cono-2. Using these equilibrium constants and K_{ov} for formation of the two disulfide bonds of α-conotoxin GI, equilibrium constants of 0.259 and 0.253 M are calculated for the second steps in which the Cys3−Cys13 and Cys2−Cys7 disulfide bonds, respectively, are formed. That is, the equilibrium constant for formation of the second disulfide bond is some 3−4 times that for formation of the first disulfide bond, which suggests a modest amount of cooperativity in formation of the second disulfide bond.

However, the equilibrium constants in Table 1 are for pH 7.00, where only a fraction of the thiol groups are in the reactive thiolate form, and thus, although they indicate some cooperativity, they may not reflect the extent of the cooperativity in terms of the reactive species. pH-independent, intrinsic equilibrium constants for the reactions in terms of thiolate species are reported in Table 5. The intrinsic equilibrium constants, K^i, were calculated from the values reported in Table 1 by accounting for the fractional thiolate

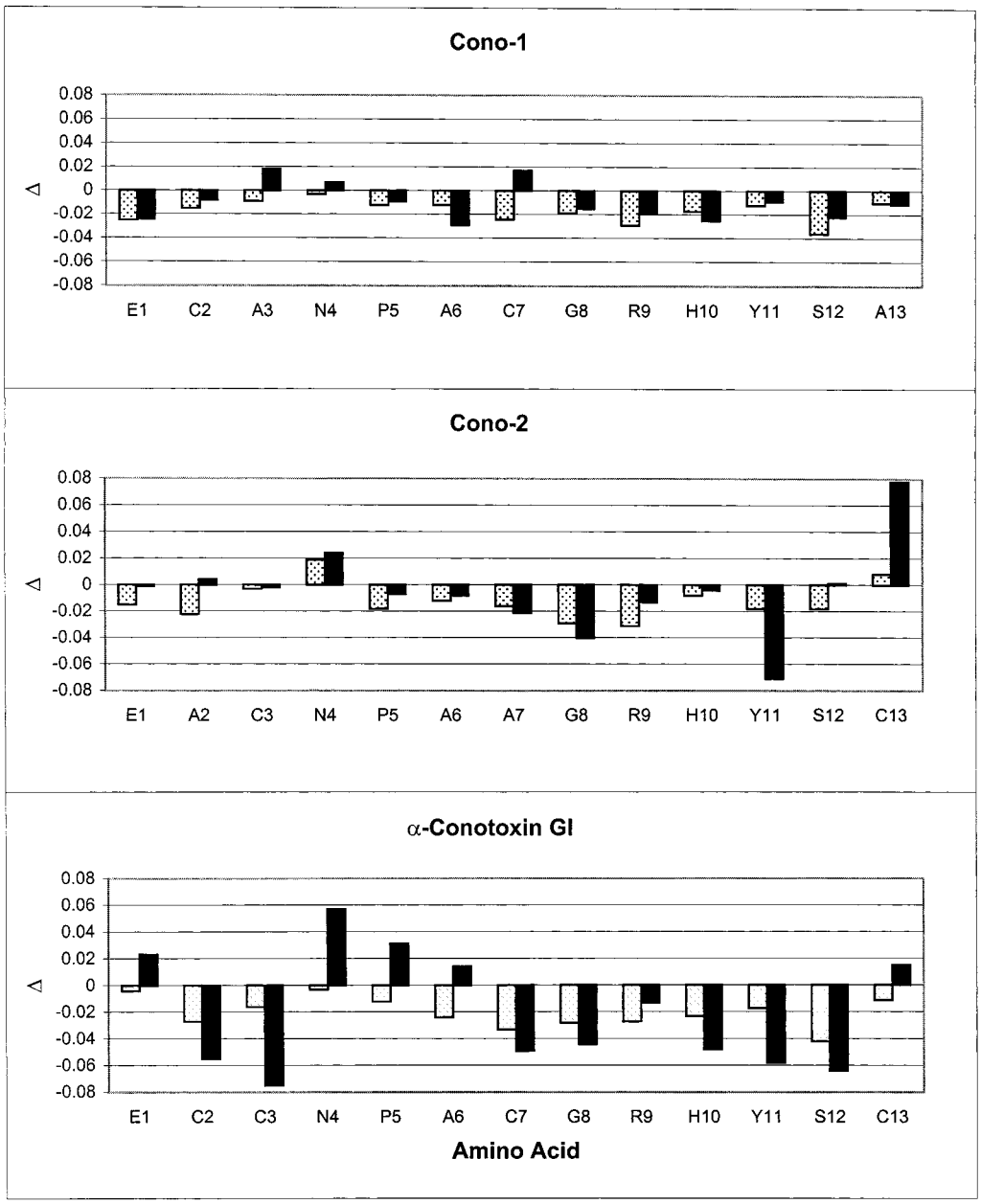

FIGURE 9: The difference between the chemical shifts of the CαH resonances of the reduced (stipled) and disulfide (black) forms of Cono-1, Cono-2, and α-conotoxin GI in 90% H_2O/10% D_2O and 90% H_2O/10% D_2O plus 8 M urea ($\Delta = \delta_{\text{no urea}} - \delta_{\text{urea}}$). pH 2.00 and 16 °C.

concentrations at pH 7.00 using the pK_A values reported in Table 4 for the thiol groups of Cono-1, Cono-2, and α-conotoxin GI and a pK_A of 8.93 for the thiol group of GSH (*30*). For example, $K_3^i = (\alpha_{GSH}^2/\alpha_2)K_3$ where α_{GSH} is the fractional concentration of GSH in the thiolate form and α_2 the fractional concentration of Cono-1 or Cono-2 in the dithiolate form at pH 7.00.

The intrinsic equilibrium constant K_3^i for formation of the disulfide bond in Cono-1 is 3 times that for formation of the disulfide bond in Cono-2, in contrast to the equal values observed for the conditional (pH 7.00) equilibrium constants (K_3). Thus, the intrinsic equilibrium constants reflect the closure of rings of somewhat different size upon formation of the disulfide bonds in Cono-1 and Cono-2. Using the values in Table 5 for K_3^i for Cono-1 and Cono-2 and K_{ov}^i for α-conotoxin GI, the intrinsic equilibrium constants for formation of the Cys3−Cys13 and Cys2−Cys7 disulfide bonds in the second step of the two-step process are calculated to be 2.1 M and 5.6 M, respectively. These values are much larger than the intrinsic equilibrium constants for formation of the first disulfide bonds of α-conotoxin GI, which indicates that, when considered in terms of the reactive thiolate species, there is a high degree of cooperativity in the formation of the second disulfide bond of α-conotoxin GI by both pathways in Figure 2.

Origin of the Cooperativity. To determine if secondary structure is the source of the cooperativity, equilibrium constants for formation of the disulfide bonds of Cono-1, Cono-2, and α-conotoxin GI by thiol/disulfide exchange were also measured in 8 M urea solution. K_3 for formation of the Cys2−Cys7 and Cys3−Cys13 disulfide bonds of Cono-1 and Cono-2, respectively, are reasonably similar in the absence and presence of urea (Tables 1 and 2). However, the equilibrium constants calculated for formation of the second

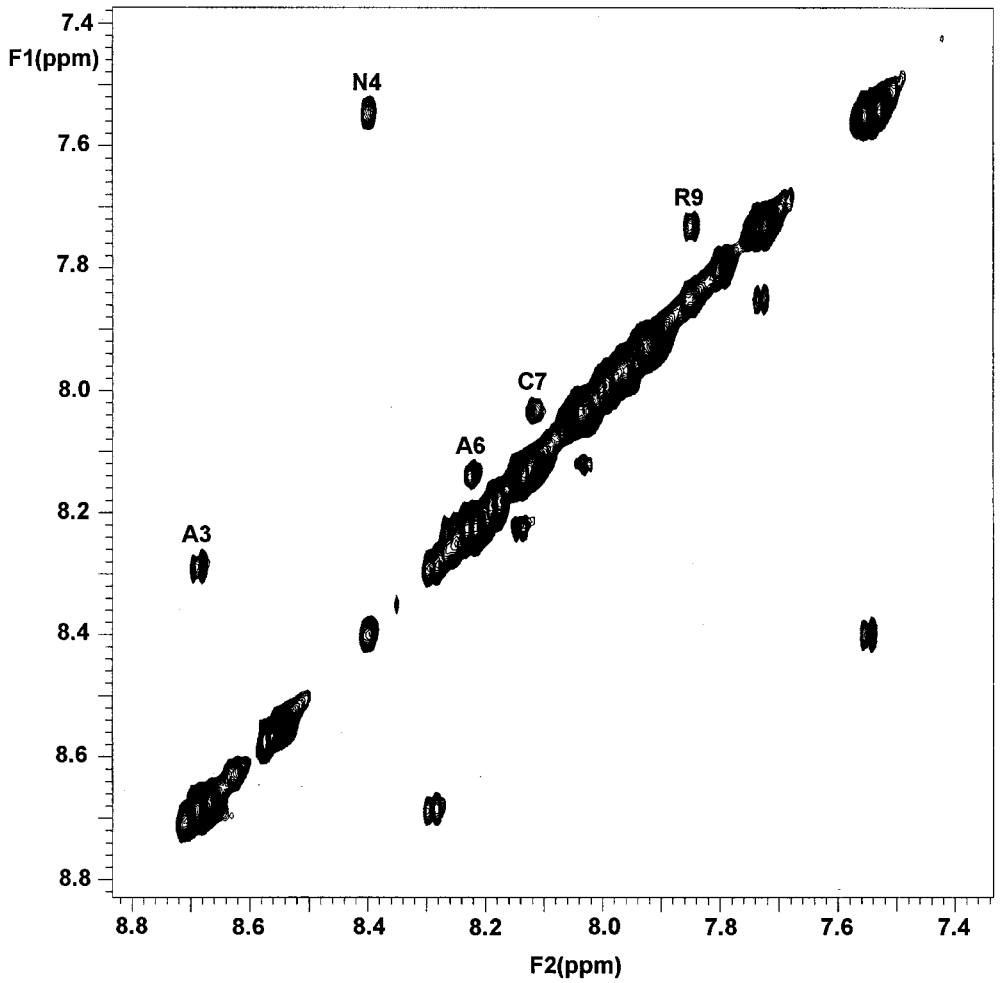

FIGURE 10: The NH−NH region of the ROESY spectrum of 6.5 mM oxidized Cono-1 in 90% H_2O/10% D_2O at pH 2.00 and 58 °C. Only the positive cross-peaks are plotted. The labeled cross-peaks are exchange cross-peaks from exchange between cis and trans conformations by rotation around the Asn4−Pro5 peptide bond.

Table 4: Group-Specific Acid Dissociation Constants for Conotoxin Peptides[a,b]

	Cono-1	Cono-2	α-Conotoxin GI
Glu1 NH_3^+	7.85 ± 0.08	7.62 ± 0.10	7.88 ± 0.11
Glu1 CO_2H	4.10 ± 0.04	3.91 ± 0.10	3.63 ± 0.10
Cys2 SH	9.09 ± 0.06		9.40 ± 0.07
Cys3 SH		9.21 ± 0.07	9.34 ± 0.04
Cys7 SH	9.14 ± 0.13		9.42 ± 0.09
His10 ImH^+	6.84 ± 0.03	6.55 ± 0.03	6.41 ± 0.05
Tyr11 OH	10.61 ± 0.02	9.91 ± 0.04	10.55 ± 0.08
Cys13 SH		8.60 ± 0.06	8.84 ± 0.09

[a] In 90% H_2O/10% D_2O at 25 °C. [b] Peptides are in the thiol form.

Table 5: Intrinsic Equilibrium Constants for Thiol/Disulfide Exchange Reactions of Cono-1, Cono-2, and α-Conotoxin GI with Glutathione

	Cono-1	Cono-2	α-Conotoxin GI
K_1^i	8.3	6.3	
K_2^i (M)	0.023	0.011	
K_3^i (M)	0.18	0.068	
K_{ov}^i $(M)^2$			0.38

disulfide bond, 0.118 and 0.174 for the Cys3−Cys13 and Cys2−Cys7 disulfide bonds, respectively, of α-conotoxin GI are smaller by approximately a factor of 2 in urea solution, which suggests that the single disulfide intermediates found on the folding pathway (Figure 2) have some secondary structure which facilitates formation of the second disulfide bonds. With this in mind, the solution structural and conformational properties of Cono-1, Cono-2, and α-conotoxin GI were investigated to identify structural features which might contribute to the cooperativity.

The solid-state X-ray structure and four solution state NMR structures have been reported for α-conotoxin GI (*10*−*14*). There is reasonable agreement between the solid-state and solution-state structures, with the differences apparently being due to crystal-packing forces in the solid state (*12*). In our discussion here, we will use the recently reported NMR structural study in which it was demonstrated that native α-conotoxin GI exists in solution as two topologically distinct interconvertible sets of conformations (populations 78 and 22%), and that interconversion between the two sets of conformations is fast on the NMR time scale (*12*). A common feature of both sets of conformations is that the Cys2−Cys7 region shows a type I β-turn over Asn4−Cys7 stabilized by a Cys7(NH)−Asn4(CO) hydrogen bond. However, the conformational properties of the Gly8−Cys13 loop of the two sets of conformations are somewhat different, with the Gly8−Cys13 loop of the major set of conformations having a helical turn from Gly8−Tyr11, while that of the minor set comprises two consecutive bends, Gly8−Arg9 and His10−Tyr11.

The NMR data reported in Table 3 and Figure 6 for α-conotoxin GI are consistent with the reported NMR solution structures. Of interest here is that the NMR data for Cono-1 and Cono-2 indicate that these two peptides, in their disulfide forms, also show some of the same secondary structure in solution. Considering first Cono-1, the Pro5-(CαH)−Cys7(NH) NOE (Figure 6) together with the Ala6-(NH)−Cys7(NH) NOE indicate a type 1 or type 2 β-turn (because Pro does not have an NH proton, it is not possible to distinguish between them) (*31*). Further evidence for an Asn4−Cys7 β-turn is provided by the small temperature dependence (Table 3) of the chemical shift of the Cys7 NH resonance. The NOE data and the temperature dependence of the amide NH chemical shifts, together with the essentially identical chemical shifts of the CαH protons (Figure 9) and the NH protons of Cys2 through Gly8 (Figure 8) in the presence and absence of urea, indicate that reduced Cono-1 is predominantly random coil. No NOE evidence for an Asn4−Cys7 β-turn was observed, which suggests that the Asn4−Cys7 β-turn in the disulfide form of Cono-1 is induced by formation of the Cys2−Cys7 disulfide bond, rather than this being a structural element which facilitates formation of the disulfide bond. This conclusion is consistent with the finding that the equilibrium constant for formation of the disulfide bond of Cono-1 is the same in pH 7.00 buffer and pH 7.00 buffer plus 8 M urea. Also, the absence of a significant change in the chemical shifts for the CαH protons (Figure 9) and the NH protons for Cys2 through Gly8 (Figure 8) of the disulfide form of Cono-1, together with temperature coefficients of 2.9 ppb/°C and 3.0 ppb/°C for the amide NH resonances of Asn4 and Cys7 of Cono-1 in 8 M urea indicate that the β-turn over Asn4−Gly8 persists in 8 M urea.

The NMR data for Cono-1 also provides evidence for other elements of secondary structure. The Ala6(CαH)−Gly8(NH) NOE together with the Ala6(NH)−Cys7(NH) and Cys7-(NH)−Gly8(NH) NOEs indicate a Pro5−Gly8 type I β-turn (*31*). Also, the NH_i-NH_{i+1} NOEs from Gly8 to Tyr11, although weak, together with the $C\alpha H_i-NH_{i+1}$ NOEs over this region suggest a small population of peptides with helical secondary structure, as found in the major set of solution conformations of α-conotoxin GI (*12*). That is, these data suggest that the Cys2−Cys7 single disulfide intermediate formed during the folding of α-conotoxin GI has elements of secondary structure present in the native structure, which might facilitate formation of the second (Cys3−Cys13) disulfide bond.

The NOE data in Figure 6 provides evidence that Cono-2 also has some of the same secondary structure as α-conotoxin GI. In particular, the Ala6(CαH)−Gly8(NH) NOE together with the weak Ala7(NH)−Gly8(NH) NOE indicates a small population of peptide having a Pro5−Gly8 β-turn. This β-turn apparently stabilizes the structure, as indicated by the small, but significant, decrease in the equilibrium constant for formation of the Cys3−Cys13 disulfide bond of Cono-2 in 8 M urea. The Pro5−Gly8 β-turn facilitates formation of the Cys2−Cys7 disulfide bond from the Cys3−Cys13 single disulfide intermediate in the folding of α-conotoxin GI.

It is clear from the NMR data, however, that although both Cono-1 and Cono-2 have some secondary structure in solution, they are both much less structured than α-conotoxin GI with its two disulfide bonds, which indicates that formation of the second disulfide bond induces considerable structure into the backbone of the peptide, which in turn stabilizes the disulfide bonds.

Redox Potentials of the Disulfide Bonds of α-Conotoxin GI. The equilibrium constants for formation of the disulfide bonds of Cono-1, Cono-2, and α-conotoxin GI by thiol/disulfide exchange with GSSG are related to the half-cell potentials for the disulfide bonds:

$$E^{\circ\prime}_{SS/SH2} = E^{\circ\prime}_{GSSG/GSH} + (RT/nF)\ln K \qquad (7)$$

The $E^{o\prime}$ values reported in Table 1 were calculated using eq 7 and $E^{\circ\prime}_{GSSG/GSH}$ (*32*). Using the values calculated above for formation of the second disulfide bonds of α-conotoxin GI from the two single disulfide intermediates, the $E^{o\prime}$values for the Cys3−Cys13 and Cys2−Cys7 disulfide bonds of the native form of α-conotoxin GI are calculated to be −0.245V and −0.244V, respectively, at pH 7.00 and 25 °C. For comparison, $E^{\circ\prime}_{SS/SH2}$ values for oxytocin and arginine vasopressin (AVP), both of which are of the general sequence C-X-X−X-X-C-X-X-X, are −0.216 V and −0.228 V, respectively, at pH 7.00 and 25 °C (*6*). The value for AVP is similar to the values for Cono-1 and Cono-2, but both are somewhat less than $E^{o\prime}$ for reduction of either disulfide bond of native α-conotoxin GI, which indicates the extra thermodynamic stability resulting from interactions which stabilize the secondary structure of α-conotoxin GI.

SUPPORTING INFORMATION AVAILABLE

^{1}H chemical shift data for the reduced and disulfide forms of Cono-1, Cono-2 and α-conotoxin GI. This material is available free of charge via the Internet at http://pubs.acs.org.

REFERENCES

1. Olivera, B. M., Gray, W. R., Zeikus, R., McIntosh, J. M., Varga, J., Rivier, J., de Santos, V. and Cruz, L. J. (1985) *Science 230*, 1338−1343.
2. Olivera, B. M., Rivier, J., Clark, C., Ramilo, C. A., Corpuz, G. P., Abogadie, F. C., Mena, E. E., Woodward, S. R., Hillyard, D. R., and Cruz, L. J. (1990) *Science 249*, 257−263.
3. Gray, W. R., Olivera, B. M., and Cruz, L. J. (1988) *Annu. Rev. Biochem. 57*, 665−700.
4. Myers, R. A., Cruz, L. J., Rivier, J. E., and Olivera, B. M. (1993) *Chem. Rev. 93*, 1923−1936.
5. Gray, W. R., Luque, A., Olivera, B. M., Barrett, J., and Cruz, L. J. (1981) *J. Biol. Chem. 256*, 4734−4740.
6. Rabenstein, D. L., and Yeo, P. L. (1994) *J. Org. Chem. 59*, 4223−4229.
7. Rabenstein, D. L., and Weaver, K. H. (1996) *J. Org. Chem. 61*, 7391−7397.
8. Gilbert. H. F. (1990) *Adv. Enzymol. 63*, 69−172.
9. Creighton, T. E. (1977) *J. Mol. Biol. 113*, 313−328.
10. Kobayashi, Y., Ohkubo, T., Kyogoku, Y., Nishiuchi, Y., Sakakibara, S., Braun, W., and Go, H. (1989) *Biochemistry 28*, 4853−4860.
11. Pardi, A., Galdes, A., Florance, J., and Maniconte, D. (1989) *Biochemistry 28*, 5494−5501.
12. Maslennikov, I. V., Sobol, A. G., Gladky, K. V., Lugovskoy, A. A., Ostrovsky, A. G., Tsetlin, V. I., Ivanov, V. T., and Arseniev, A. S. (1998) *Eur. J. Biochem. 254*, 238−247.
13. Gehrmann, J., Alewood, P. F., and Craik, D. J. (1998) *J. Mol. Biol. 278*, 401−415.
14. Guddat, L. W., Martin, J. A., Shan, L., Edmundson, A. B., and Gray, W. R. (1996) *Biochemistry 35*, 11329−11335.
15. Carpino, L. A. (1993) *J. Am. Chem. Soc. 115*, 1497−1498.
16. Angell, Y. M., Garcia-Echeverria, C., and Rich, D. H. (1994) *Tetrahedron Lett. 35*, 5981−5984.

17. King, D. S., Fields, C. G., and Fields, G. B. (1990) *Int. J. Pept. Protein Res. 36*, 255−266.
18. Ferrer, M., Woodward, C., and Barany, G. (1992) *Int. J. Pept. Protein Res. 40*, 194−207.
19. Tam, J. P., Wu, C. R., Liu, W., and Zhang, J. W. (1991) *J. Am. Chem. Soc. 113*, 6657−6662.
20. Munson, M. C., and Barany, G. (1993) *J. Am. Chem. Soc. 113*, 10203−10210.
21. States, D. J., Haberkorn, R. A., and Ruben, D. J. (1982) *J. Magn. Reson. 48*, 286−292.
22. Rabenstein, D. L., Hari, S. P., and Kaerner, A. (1997) *Anal. Chem. 69*, 4310−4316.
23. Huyghues-Despointes, B. M. P., and Nelson, J. W. (1992) *Biochemistry 31*, 1476−1483.
24. Chau, M.-H., and Nelson, J. W. (1992) *Biochemistry 31*, 4445−4450.
25. Xu, X., and Nelson, J. W. (1994) *Biochemistry 33*, 5253−5261.
26. Larive, C. K., Guerra, L., and Rabenstein, D. L. (1992) *J. Am. Chem. Soc. 114*, 7331−7337.
27. Wishart, D. D., Sykes, B. D., and Richards, R. M. (1991) *J. Mol. Biol. 222*, 311−333.
28. Bothner-By, A. A., Stephens, R. L., Lee, J., Warren, C. D., and Jeanloz, R. W. (1984) *J. Am. Chem. Soc. 106*, 811−813.
29. Zhang, R., and Snyder, G. H. (1991) *Biochemistry 30*, 11343−11348.
30. Rabenstein, D. L. (1973) *J. Am. Chem. Soc. 95*, 2797−2803.
31. Wüthrich, K. (1986) *NMR of Proteins and Nucleic Acids*, John Wiley & Sons, New York.
32. Millis, K. K., Weaver, K. H., and Rabenstein, D. L. (1993) *J. Org. Chem. 58*, 4144−4146.

BI9826658